KOM
CORROSION AND MATERIAL PROTECTION JOURNAL

ORIGINAL ARTICLE

sciendo

Synthesis and study of corrosion behavior of terephthalaldehyde-derived schiff base for low-carbon steel in HCl: experimental, morphological and theoretical investigation

Betti N.[1], Al-Azzawi W.K.[2], Alamiery A.[3]
[1] Materials Engineering Department, University of Technology-Iraq, Baghdad, Iraq
[2] Al-Farahidi University, Baghdad, Iraq
[3] Department of Chemical and Process Engineering, Faculty of Engineering and Built Environment, Universiti Kebangsaan Malaysia Bangi, Selangor, Malaysia
E-mail: dr.ahmed1975@ukm.edu.my

In the present investigation, corrosion inhibition assays of the terephthalaldehyde-derived Schiff base of low-carbon steel have been performed in a 1.0 mol L^{-1} hydrochloric acid solution. Weight loss measurements were applied to investigate the corrosion inhibition efficacy of Schiff base as an inhibitor. The highest inhibitive efficacy was achieved at a select concentration of 500.0 ppm for the tested inhibitor. The Langmuir adsorption isotherm model was applied to portray the adsorption inhibition mechanism. The variation in the activation energy value in the presence of synthesized inhibitor indicates the types of interactions between the inhibitor molecules and low-carbon steel surface. Scanning electron microscopy analyses proved the adsorption of inhibitor molecules on the low-carbon steel surface and through form a film that protects the metallic surface from corrosion. Furthermore, the relationship between inhibitive efficacy and the inhibitor molecule structure was studied theoretically through density functional theory (DFT). The experimental and theoretical findings reveal compatible harmony between them.

INTRODUCTION

Low-carbon steel surface corrosion protection has brought important concern due to extensive economic and safety losses as a consequence of corrosion in different applications. Many manufacturers use low-carbon steel as an important type of substance as it is widely utilized and has different utilization, gratitude to the low cost and excellent mechanical and engineering characteristics [1-5]. Despite, its compelling application, low-carbon steel applied in manufacturers is readily exposed to corrosion, especially in hydrochloric acid solution. Thus, due to low corrosion resistance, it is important to find specific techniques to protect the surface of low-carbon steel from acidic solutions and corrosion. Amongst different possible approaches, an example of the extensively utilized strategies is using natural or synthetic organic molecules as inhibitors for decreasing and controlling corrosion in corrosive environments [6-9]. Various heterocyclic molecules having heteroatoms such as phosphorous, sulfur, oxygen, and nitrogen, and also containing pi-bond systems show remarkable corrosion inhibition achievement [10,11]. Natural and synthetic organic molecules of such a species are readily adsorbed on the lo-carbon steel surface due to the unpaired lone pairs of electrons and also pi-system with the alloy surface, consequently reducing or controlling the corrosion [12,13]. In recent years, imine or azomethine (−N=CH) group which named Schiff base, producing from the reaction of carbonyls and primary or amines, as a significant corrosion inhibitor has gained a great deal of interest by investigators [14-18]. Corrosion inhibitors containing together sulfur and nitrogen atoms are very effective in inhibiting corrosion unlike corrosion inhibitors containing one type of heteroatoms [19]. Thiadiazoles are one of these classes of compounds containing both nitrogen and sulfur for which Schiff bases have been published and the effect of these molecules on corrosion inhibition has been verified [20,21]. The non-cytotoxic characteristics of thiadiazoles make them ecofriendly corrosion inhibitors [22-25]. In continuation of the investigation on improvement of organic compounds as efficient corrosion inhibitors in hydrochloric acid solution, the present study presents the inhibition efficiency of terephthalaldehyde Schiff base, namely, 4-{[(5-ethyl-1,3,4-thiadiazol-2-yl)imino] methyl}benzaldehyde (ETIMB) on corrosion of low-carbon steel in 1.0 mol L^{-1} hydrochloric acid by using gravimetric methods, and scanning electron microscopy (SEM) analysis. In order to understand the mechanism of adsorption of inhibitor molecules on the low-carbon steel

surface, various adsorption isotherms were presented. Langmuir adsorption isotherm was accounted to be quite agreeable to clear the inhibitor molecules adsorption process on the low-carbon steel surface. The effectiveness of temperature variation with various inhibitor concentrations is investigated. Density functional theory (DFT) was utilized to elucidate the efficient interaction mechanism of the inhibitor molecules with the surface of low-carbon steel. All the results are agreed with the computational calculations.

EXPERIMENTAL

Steel sampling

Type low-carbon steel coupons having 0.21 % Carbon, 0.09 % Phosphorus, 0.05 % Manganese, 0.038 % Silicon, 0.01 % Aluminum, 0.05 % Sulfur and the remainder Iron was utilized. Prior to every experiment, the low-carbon steel coupons were split into various areas, cleaned with sandpaper, degreased with acetone, and collected in the oven before treatment [21, 22] to block the coupons from air humidity. Ready coupons were hung with the assistant of wire in a beaker containing 250 ml of 1 mol L^{-1} HCl (37%) in the presence and absence of ETIMB as a tested inhibitor. Each sample following corrosion examination was washed with double distilled water, dipped in methyl alcohol to eliminate ETIMB particles and chlorine residual, immersed in acetone, and finally dried in an oven and reset weights.

Synthesis of Inhibitor

The ETIMB was synthesized by refluxing terephthaldehyde (0.005 mol) with 2-amino-5-ethyl-1,3,4-thiadiazole (0.004 mol), that is, 1:1 molar ratio in ethyl alcohol (50 mL) using glacial acetic acid as a catalyst for 9 h,. The dark yellow solid precipitate therefore collected was filtered and dried. ETIMB as a synthesized corrosion inhibitor was re-crystallized using ethyl alcohol to achieve a purified compound (Yield 49% and M.P. 168-172 °C).

Weight loss analyses

Gravimetric analysis was performed on low-carbon steel coupons in 1mol L^{-1} HCl medium in the presence and absence of ETIMB. Primary measurements of the polished coupons were listed. The coupons were exposed to the analysis liquid utilizing a glassful clamp in triplicate in the presence and absence of ETIMB. The coupons were reweighed after removed, rinsed with water, and dried. The time effect on the inhibition efficiency at various inhibitor concentrations was investigated on the period (1, 5, 10, 24, and 48 h). The temperature effect on the inhibition efficacy at various concentrations was investigated on the scale (303-333 K). The temperature of the examined solution was regulated by the thermostat selector at the wanted temperature. The values of rate of corrosion (C_R; mm y^{-1}) and inhibition efficacy (IE %) were determined utilizing Equations. 1 and 2 individually

$$C_R = \frac{87.6\ W}{DAT} \tag{1}$$

$$IE = \frac{C_{Ro} - C_R}{C_{Ro}} \quad (\%) \tag{2}$$

where W is the loss in coupon weight, A represents the immersion area, D refer to the coupon density, T is immersion period and finally C_{Ro} and C_R refer to the values of the rates of corrosion without and with the corrosion inhibitor respectively.

Surface morphology investigation

The coupon surface morphology which was exposed to 1 mol L^{-1} HCl in the presence and absence of ETIMB was investigated at room temperature by scanning electron microscope (SEM) to examine the coupon surface before and after the weight loss measurements. The difference in the low-carbon steel surface was examined by the Scanning Electron Microscope (TM1000 Hitachi Tabletop Microscope SEM). The tested coupon was exposed to 1 mol L^{-1} HCl solution for 5 h without and with the optimum inhibitor concentration. Moreover, the examined coupons were taken away, washed with deionized water, dried, and examined by SEM.

Theoretical investigations

To probably explain the issue of the inhibitor's performance and to recognize the common important factors that may control the inhibitive efficacy, herein, we performed quantum chemical computations. The theoretical factors were evaluated and ascertained by Density function theory (DFT). To study the electronic characteristics of the examined inhibitor molecules, Becke's three-parameter hybrid functional utilizing the LYP correlation functional (B3LYP) was conducted [26,27]. The energy of ionization and the affinity were evaluated utilizing the highest energy MO (HOMO) and lowest energy MO (LUMO) and from which, the electronegativity and hardness were determined [28].

$$\text{Ionization energy (I)} = -E_{\text{HOMO}} \tag{3}$$

$$\text{Electronic affinity (A)} = -E_{\text{LUMO}} \tag{4}$$

$$\text{Electronegativity } (\chi) = \frac{I + A}{2} \tag{5}$$

$$\text{Hardness } (\eta) = \frac{I - A}{2} \tag{6}$$

Transferred electrons fraction (ΔN) was determined [29] according to Equation (7),

$$\Delta N = \frac{\phi - \chi_{inh}}{2(\eta_{Fe} + \eta_{inh})} \quad (7)$$

The iron work function (ϕ) was essentially taken as 4.82 eV, whereas the iron hardness was evaluated at 0 as $I = A$ [30].

RESULT AND DISCUSSION

Chemistry of the inhibitor

Schiff base (ETIMB) is typically synthesized by the condensation reaction of a primary amine (2-amino--5-ethyl-1,3,4-thiadiazole) and an aldehyde (terephthaldehyde) which involves the use of ethanol as solvent. The excess of terephthaldehyde was owing to directing the condensation reaction towards attacking one carbonyl group of terephthaldehyde, as per the Scheme displayed in Figure 1.

Effect of Inhibitor Concentration

The value of corrosion rate was very high in absence of the studied inhibitor, and suddenly it begins to reduce steadily with the addition of the studied inhibitor to the tested solution as exhibited in Figure 2. However, inhibitive efficacy increases with an increase in the studied inhibitor concentration through straight relation as shown in Figure 2. The increase in studied inhibitor concentration reaches to increases the adsorption of the inhibitor molecules and also the surface coverage, and hence, resulting in a decrease in rate of corrosion

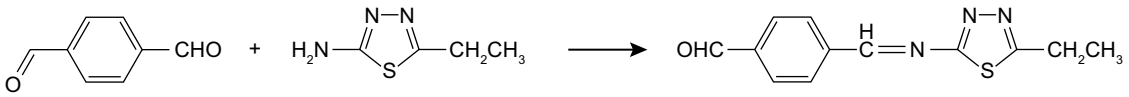

Fig. 1. A plot of synthesis of ETIMB as a corrosion inhibitor

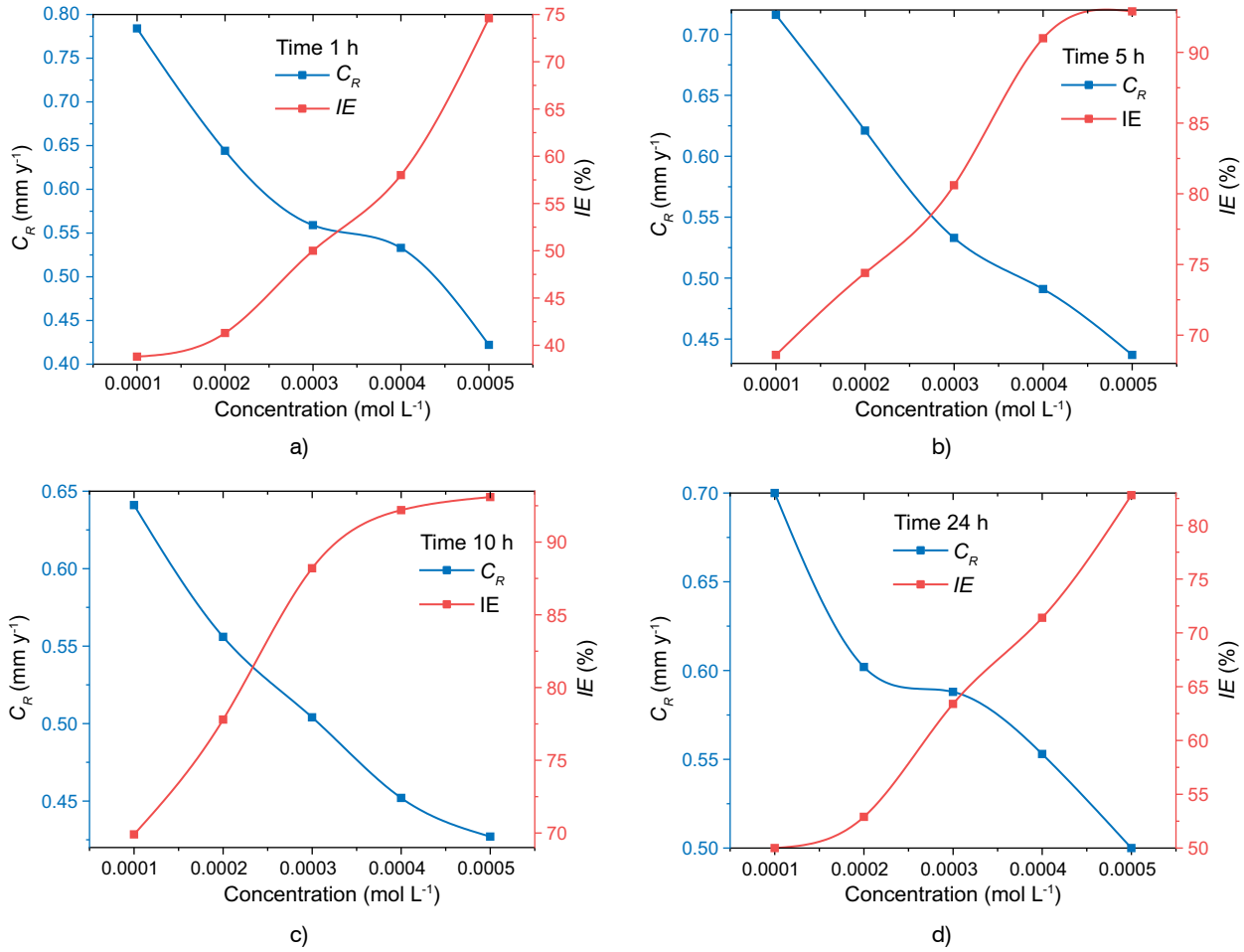

Fig. 2. Weight loss effects of low-carbon steel in 1.0 mol L^{-1} HCl with various concentrations of ETIMB at various immersing time

value. The experimental findings indicate that the rate of corrosion value reduction with the addition of inhibitor at the investigated concentrations [30-35].

Effect of immersion time

The obtained experimental findings reveal that the exposure period becomes an important effect on the rate of corrosion, particular weight loss, inhibitive efficacy, and the surface coverage degree. Figure 2 presents the difference in mass loss with the exposure period. Figure 2, demonstrated that the gravimetric result of corrosion rate increases with the exposure period for tested coupons. However, the mass loss value reported by the inhibited specimens reduces with a concentration of synthesized inhibitor increase. Therefore, the increase in mass loss observed during the immersion period in the hydrochloric acid solution, may have caused the low carbon steel to be "wet" for a continuous period. Moreover, Figure 2 presents the scheme of the inhibitive efficacy versus time and also reveals the rate of corrosion with time. The experimental findings show that the inhibitive efficacy decrease as immersion time is remarkably increased for all utilized concentrations of tested inhibitor. The decrease in inhibitive efficacy with immersion time was imputed to the reacting of inhibitor (ETIMB) molecules with an environment species resulting in loss of inhibitor or exhaustion over time due to chemical reactions taking place within the environment. The reduction in inhibitive efficacy for a long exposure period may be due to the deficiency of free inhibitor molecules in the system due to metal complex formation between the d-orbital of iron atoms on the low-carbon steel surface and the unpaired pairs of electrons of the inhibitor molecules. Therefore, there might be a decrease in inhibitive efficacy with the exposure period owing to desorption. The highest inhibition activity was 92.9 % after the immersion time (5 hours), with a concentration of 500 ppm of ETIMB, and increasing the concentration more than that did not lead to a significant difference in the inhibition activity within the range of inhibitor concentration examined. This comment may perhaps be attributed to the inhibitive efficacy leading a saturation point after 500 ppm concentration of ETIMB. It might also be due

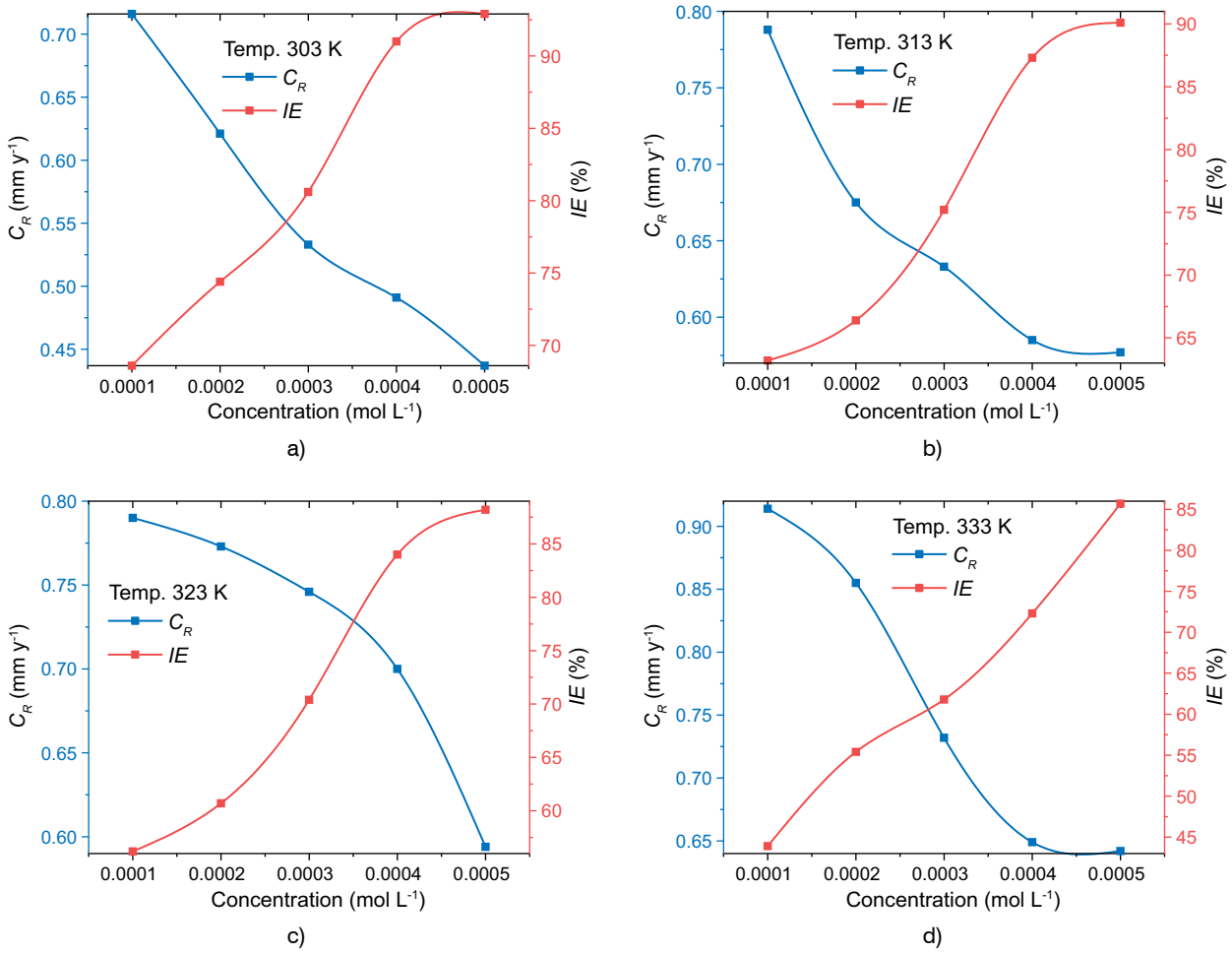

Fig. 3. Weight loss effects of low-carbon steel in 1.0 mol L^{-1} HCl with various concentrations of ETIMB at various temperatures for 5 h as exposure time

to the competing adsorption influence between ETIMB molecules and the alloy surface which is previously treated with the initial film of the ETIMB molecules.

Impact of temperature

The impact of temperature was investigated on the corrosion rate and inhibition efficiency. The achieved outcomes are presented in Figure 3. Generally, the value of the rate of corrosion was observed to increase with rising temperature as exhibited in Figure 3. The more important temperature effect is to expedite chemical interaction and to decrease the solubility of oxygen, which enables the existence of cathode reactions. Figure 3 also indicates the effect of the inhibitor with a de-crease in the low-carbon steel coupon value of the rate of corrosion. The temperature has a negative impact on the inhibitive efficacy, a rise in temperature leads to an accretion of the dynamic energy for the tested inhibitor molecules. The accretion in dynamic energy reduces the protecting layer formed on the surface of the low-carbon steel coupon. Besides raising in temperature, the inhibition efficacy decreased from 92.9% to 85.7%.

Adsorption isotherm

Based on the inhibitor molecules' adsorption on the surface of low-carbon steel, significant data is offered using various adsorption isotherm models. Langmuir isotherm was considered to be the common agreeable one to confirm the adsorption of the tested inhibitor on the surface of low-carbon stee because the linear regression coefficient is recognized so close to unity [29]. Langmuir isotherm model is fully described according to Equation (8).

$$\frac{C_{\text{inh}}}{\theta} = \frac{1}{K_{ads}} + C_{\text{inh}} \tag{8}$$

This relationship summarizes the dependence of the inhibitor concentration with the surface coverage (θ). The coverage of surface is described as the section of the surface treated by an molecules of tested inhibitor and can be determined according to Equation (9).

$$\theta = \frac{W_o - W_i}{W_o} \tag{9}$$

The plot of C_{inh}/θ against C_{inh} achieved at 303 K provides a straight line, therefore, inhibitor molecules adsorption obey Langmuir adsorption model further correctly as matched to other adsorption isotherm models. K_{ads} implies affinity between the adsorbate and adsorbent. K_{ads} with the highest value indicated more excellent adsorption and finally process more reliable inhibition efficiency [36-40]. K_{ads} can be determined utilizing the intercept of the straight line (Figure 4). The relationship between the adsorption free energy and adsorption equilibrium constant can be describes according to Equation (10).

$$\Delta G^{\circ}_{\text{ads}} = -RT \ln (55.5\ K_{\text{ads}}) \tag{10}$$

where R represents the universal gas constant, T refers to the absolute temperature, and K_{ads} is the adsorption equilibrium constant.

The adsorption free energy ($\Delta G^{\circ}_{\text{ads}}$) with negative value implies that the adsorption process is spontaneity; that is the inhibitor molecules are efficiently adsorbed on the surface of lo-carbon steel [41-44]. It is obvious that the physisorption of the inhibitor molecules to the surface of coupon is identified by ($\Delta G^{\circ}_{\text{ads}} \leq -20$ kJ/mol). But, a adsorption free energy with extremely negative value ($\Delta G^{\circ}_{\text{ads}} > -40$ kJ/mol) implies a chemisorption via coordination bonds between unocupied d-orbitals of iron atoms on the coupon surface and unshred pairs of electrons of tested inhibitor molecules [45-48]. In this illustration, $\Delta G^{\circ}_{\text{ads}}$ value is determined as −38.7 kJ/mol for studied inhibitor. This implies that the mechanism of inhibition suggests chemisorption and physisorption, mixed interaction type.

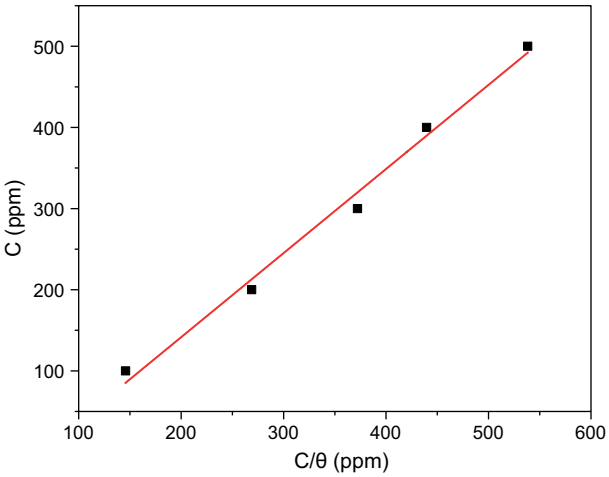

Fig. 4. Langmuir adsorption isotherm of ETIMB on the low-carbon steel surface in 1 mol L^{-1} HCl at 303 K

Computational studies

The molecular reactivity of the investigated inhibitor molecules was studied and distinguished by the study of HOMO and LUMO molecular orbitals (MOs). The HOMO energy is related to the ability of electron donation of inhibitor molecules. HOMO energy with high values of the state that the particle is likely to give electron pairs to suitable acceptor element which has unoccupied molecular orbital. Moreover, the level of energy of LUMO is a pointer to the ability of a molecule to accepting an electron. It is significant to remark that the molecule with a low energy value of LUMO has a higher ability for accepting electron ability. The

reactivity of inhibitor molecule is supposed to be nearly associated with the HOMO and LUMO molecular orbitals. The frontier MO density distribution concerning the optimum molecular structure, EHOMO and ELUMO of the studied inhibitor molecule (ETIMB) are exhibited in Figure 5. The non-protonated ETIMB molecules were investigated by DFT to determine the optimum molecular structure, EHOMO and ELUMO as revealed in Figure 5. As observed in Figure 5, the HOMO populations concentrated around the heterocyclic ring and −N=C− group. Although the densities of LUMO were generally around the benzene ring. The molecule with the high energy of HOMO suggests a more important ability to donate electrons to suitable element have vacant molecular orbital with low-energy and hence describes the adsorption of inhibitor molecules on low-carbon steel surface. The energy of LUMO means the tendency to receive electrons. HOMO with a high energy value is possible to symbolize a tendency to donating-electron a suitable element that has low-energy unoccupied d-orbital molecules. Theoretical chemical characteristics including HOMO, LUMO, energy gap (ΔE = HOMO – – LUMO), hardness, softness, electronegativity, and affinity are significant and valuable parameters to correlate the corrosion inhibitive efficacy of inhibitor molecules. Computed quantum chemical factors of the tested inhibitor are displayed in Table 1. It is obvious from Table 1 that ETIMB molecules have a high value of HOMO energy whereas. This suggests that the ability to donate electrons of ETIMB is high. This endorses the experimental findings that the interaction of ETIMB and iron atoms on the surface is physisorption. The LUMO energy is associated with the affinity of electrons and describes the molecule's susceptibility to nucleophilic attack. LUMO, with low-value energy a more powerful ability to accept an electron. Low values of the energy gap (ΔE) will provide good inhibitive efficiency cause the energy of excitation which demands to eliminate an electron from the orbital would below [49-52]. The chemical hardness (η) is determined as energy gap/2 and chemical softness was also evaluated. These factors also present data about the molecule's reactive performance and are exhibited in Table 1. A molecule with a low ΔE is higher polarizable and is usually correlated with a great chemical reactivity and low dynamic stability, and is named soft molecule [53-55]. The inhibitor molecules' adsorption on the surface of tested coupons happens at the role of the molecule which has the highest softness and lowest hardness. The computed outcomes explain that ETIMB molecules have low values of ΔE and hardness; this agrees with the laboratory findings that ETIMB molecules could have significant inhibition efficacy on low-carbon steel surface, through physisorption adsorption mechanism (electrostatic interaction). ETIMB molecules had significant inhibitive efficacy due to the high energy value of HOMO which

Tab. 1. Quantum chemical factors for the synthesized inhibitor molecule employing DFT calculations

Inhibitor	ETIMB
I	8.274 eV
A	5.152 eV
E_{HOMO}	–8.274 eV
E_{LUMO}	–5.152 eV
ΔE	3.122 eV
χ	6.723 eV
η	–1.561 eV
ΔN	0.017

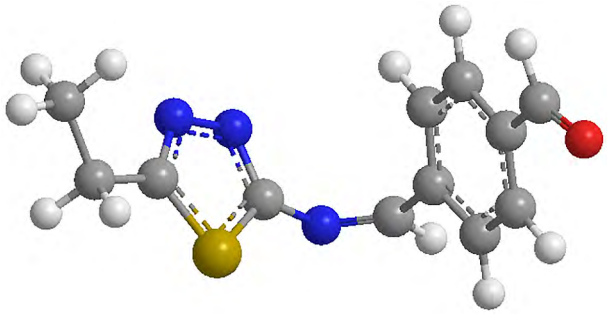

a) Optimized structure

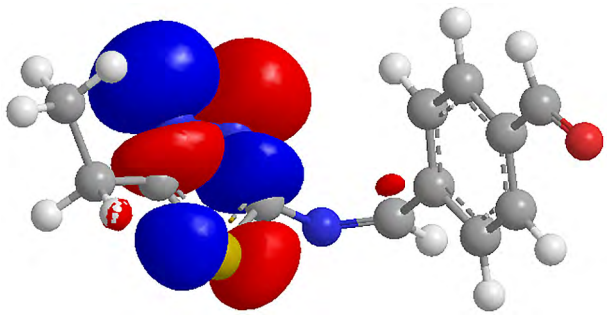

b) HOMO

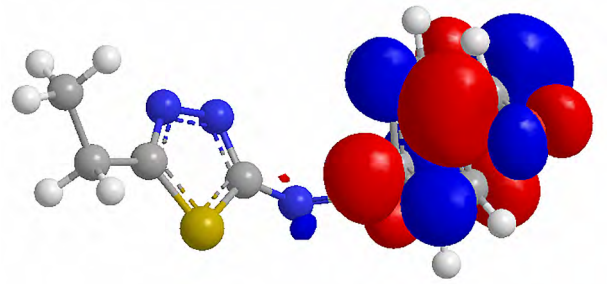

c) LUMO

Fig. 5. The optimized structure, HOMO and LUMO MOs for the synthesized Inhibitor molecule employing DFT calculations

offers the most excellent abilities to offer electrons. This also matches completely with the value of (ΔG^{o}_{ads}) realized from the adsorption isotherm. The molecular structure can influence the adsorption by determining the electron density at the active site. Usually, electrophilic attacks of the particles at negatively charged positions. As observed from Figure 5, the density of electrons concentrated on sulfur, oxygen, and nitrogen atoms. The highest electron density regions are commonly the positions to which electrophiles are attacked. So, sulfur, oxygen, and nitrogen atoms were the active sites, which had the most powerful strength of bonding to the steel surface. Electronegativity is a significant factor in the prediction of inhibitive efficacies of inhibitors. The number of electrons transferred between the element and inhibitor molecules was determined according to Equation (7). It is recognized from Eq. (7), that the electron transfer value element and inhibitor molecules reduce as the inhibitor electronegativity increases. The electron transfer between steel and inhibitor molecules remains continuously the values of electronegativities fit equal with each other. The interactions of acceptor-donor were estimated through the number of transferred electrons from the inhibitor molecules to the d-orbital of iron atoms on the coupon surface. ΔN with a positive value indicates the inhibitor molecule's ability to donor its electrons and vice-versa for a negative value, and it ordinarily obeys the EHOMO [56-62].

Surface Analysis

The differences that occur on the tested coupon surface were examined in 1 mol L^{-1} HCl in the without and with ETIMB after a 5 h exposure period and are presented in Figures 6a and 6b. The coupon surface exposed in the HCl solution without the addition of inhibitor observes obvious corrosion holes on the tested coupon surface owning to generalized corrosion damage effected by the acidic solution. The corrosion damage is seen to be missing from the coupon surface in the presence of ETIMB in the acid solution (Figure 6b). The tested coupon surface immersed in a corrosive medium with the ETIMB is remarked to be quite similar to that of the polished. This implies that the shielding film of the inhibitor molecules on the steel surface represents a barrier against corrosive solution attack.

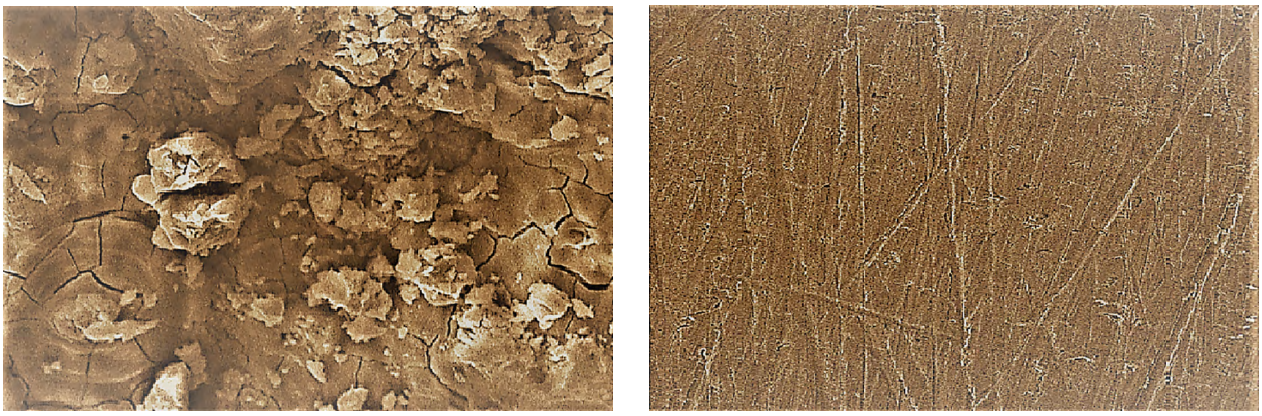

a) b)

Fig. 6. SEM photographs of low-carbon steel in 1 mol L^{-1} HCl solution exposed for 5 h: a) without inhibitor, b) with 500 ppm ETIMB

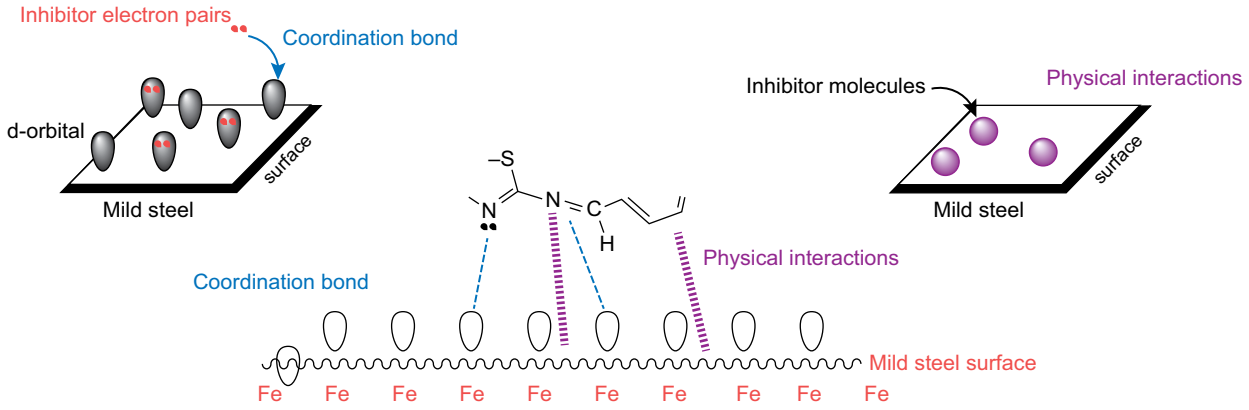

Fig. 7. Suggested inhibition mechanism for mild steel by ETIMB molecules displayed chemisorption and physisorption

Mechanism of inhibition

The corrosion of low-carbon steel in a corrosive solution having ETIMB can be controlled because of the adsorption of ETIMB molecules through it unpaired electron pairs which interact with the unoccupied d-orbital of Fe atoms of the coupon surface. Sulfur, oxygen, and nitrogen as heteroatoms of the ETIMB molecules represent the reaction sites in the adsorption process. Since the computed $\Delta G^{o}_{ads} = -38.7$ kJ/mol, it is obvious that the interactions of inhibitor molecules with low-carbon steel surface is either physisorption (electrostatic interactions) and chemosorption (chemical reaction). Since discussed earlier, the inhibition of low-carbon steel is principally guaranteed due to having the heteroatoms. The generation of the protective layer was recognized owing to the inhibitor molecules adsorption on the low-carbon steel surface. Figure 7, showed the various adsorption modes of adsorbed ETIMB molecules on the steel/HCl interface.

CONCLUSIONS

The corrosion inhibition and adsorption investigations of synthesized new inhibitor on low-carbon steel surface in 1 mol L^{-1} HCl were investigated. The result reveals the following:

- The presence of heteroatoms acts as an active site for the adsorption process on the low-carbon steel surface.
- The inhibitive efficacy of the low-carbon steel surface in 1 mol L^{-1} HCl solution increases with the increase in the concentration of the tested inhibitor. The highest inhibition efficacy of 92.9% was obtained for 500 ppm of tested inhibitor. This action was found to be due to the production of a protected film on the metal/electrolyte interface
- Based on weight loss techniques, an increase in solution Temperature will decrease the inhibition efficiency.
- The adsorption process obeyed the Langmuir adsorption model. The negative value of *ΔGads* assumes that the adsorption process was mixed with physisorption and chemisorption.
- The surface morphology investigations of the low-carbon steel surface by SEM also assume the form of a protected layer that covers the surface of low-carbon steel.
- All the experimental results were in fine agreement with the theoretical investigations. DFT efficiently described the relationship of the inhibitive efficacy with the molecular structure of the tested inhibitor.
- Therefore, the overall findings assume that the tested inhibitor can be efficiently utilized as a corrosion inhibitor for low-carbon steel in hydrochloric acid solution.

Acknowledgments

The authors are grateful to the University Kebangsaan Malaysia (UKM) for support.

REFERENCES

1. Salman, T.A. et al. A Study on the Inhibition of Mild Steel Corrosion in Hydrochloric Acid Environment by 4-Methyl-2-(Pyridin-3-Yl)Thiazole-5-Carbohydrazide. *International Journal of Corrosion and Scale Inhibition* **2019**, 8 (4).
2. Al-Amiery, A.A., A.A.H. Kadhum, A.B. Mohamad, and S. Junaedi. A Novel Hydrazinecarbothioamide as a Potential Corrosion Inhibitor for Mild Steel in HCl. *Materials* **2013**, 6 (4).
3. Kadhum, A.A.H. et al. Corrosion of Nickel-Aluminum-Bronze Alloy in Aerated 0.1 M Sodium Chloride Solutions under Hydrodynamic Condition. *International Journal of Electrochemical Science* **2013**, 8 (4).
4. Al-Amiery, A.A., Y.K.A. -Majedy, A.A.H. Kadhum, and A.B. Mohamad. New Coumarin Derivative as an Eco-Friendly Inhibitor of Corrosion of Mild Steel in Acid Medium. *Molecules* **2015**, 20 (1).
5. Musa, A.Y. et al. Quantum Chemical Calculation for the Inhibitory Effect of Compounds. *Journal of Structural Chemistry* **2013**, 54 (2).
6. Braihi, A.J. et al. Chemical Resistance of N/SB Rubber Blends for Surfaces Corrosion Protection of Metallic Tanks in Petrochemical Industries. *Koroze a Ochrana Materialu* **2020**, 64 (2).
7. Jawad, Q.A. et al. Synthesis, Characterization, and Corrosion Inhibition Potential of Novel Thiosemicarbazone on Mild Steel in Sulfuric Acid Environment. *Coatings* **2019**, 9 (11).
8. Al-Amiery, A.A. et al. Novel Corrosion Inhibitor for Mild Steel in HCl. *Materials* **2014**, 7 (2).
9. Issa, A.Y., K.S. Rida, A.Q. Salam, and A.A. Al-Amiery. Acetamidocoumarin as a Based Eco-Friendly Corrosion Inhibitor. *International Journal of ChemTech Research* **2016**, 9 (11).
10. Gaaz, T.S. et al. 2020. Evaluation of Green Corrosion Inhibition by Extracts of Citrus Aurantium Leaves against Carbon Steel in 1M HCl Medium Complemented with Quantum Chemical Assessment. *International Journal of Thin Film Science and Technology* **2020**, 9 (3).
11. Resen, A. M. et al. Exploration of 8-Piperazine-1-Yl-methylumbelliferone for Application as a Corrosion Inhibitor for Mild Steel in Hydrochloric Acid Solution. *International Journal of Corrosion and Scale Inhibition* **2021**, 10 (1).
12. Obayes, Hasan R et al. 2014. Quantum Chemical Assessment of Benzimidazole Derivatives as Corrosion Inhibitors. *Chemistry Central Journal* **2014**, 8 (1).
13. Salman, T.A. et al. Novel Ecofriendly Corrosion Inhibition of Mild Steel in Strong Acid Environment: Adsorption Studies and Thermal Effects. *International Journal of Corrosion and Scale Inhibition* **2019**, 8 (4).
14. Al-Amiery, A.A. et al. Inhibition of Mild Steel Corrosion in Sulfuric Acid Solution by New Schiff Base. *Materials* **2014**, 7 (2).

15. Alamiery, A. et al. A Study of Acidic Corrosion Behavior of Furan-Derived Schiff Base for Mild Steel in Hydrochloric Acid Environment: Experimental, and Surface Investigation. *Materials Today: Proceedings* **2021**, 44.
16. Eltmimi, A J M, A Alamiery, A J Allami, and R M Yusop. Inhibitive Effects of a Novel Efficient Schiff Base on Mild Steel in Hydrochloric Acid Environment. *International Journal of Corrosion and Scale Inhibition* **2021**, 4 (2).
17. Al-Baghdadi, Shaimaa B. et al. Anticorrosion and Antibacterial Effects of New Schiff Base Derived from Hydrazine. *Journal of Physics: Conference Series* **2021**, 1795 (1).
18. Al-Amiery, Ahmed et al. Quantum Chemical Elucidation on Corrosion Inhibition Efficiency of Schiff Base: DFT Investigations Supported by Weight Loss and SEM Techniques. *International Journal of Low-Carbon Technologies* **2020**, 15 (2).
19. Al-Azawi, K.F. et al. Experimental and Quantum Chemical Simulations on the Corrosion Inhibition of Mild Steel by 3-((5-(3,5-Dinitrophenyl)-1,3,4-Thiadiazol-2-Yl)Imino) Indolin-2-One. *Results in Physics* **2018**, 9.
20. Salman, T.A. et al. Effect of 1,3,4-Thiadiazole Scaffold on the Corrosion Inhibition of Mild Steel in Acidic Medium: An Experimental and Computational Study. *Journal of Bio- and Tribo-Corrosion* **2019**, 5 (2).
21. Junaedi, S. et al. Synthesis and Characterization of Novel Corrosion Inhibitor Derived from Oleic Acid: 2-Amino 5-Oleyl-1,3,4-Thiadiazol (AOT). *International Journal of Electrochemical Science* **2012**, 7 (4).
22. Junaedi, S. et al. Synthesis and Characterization of Novel Corrosion Inhibitor Derived from Oleic Acid: 2-Amino 5-Oleyl-1,3,4-Thiadiazol (AOT). *International Journal of Electrochemical Science* **2012**, 7 (4).
23. Salman, Abbas Z. et al. Selected BIS-Thiadiazole: Synthesis and Corrosion Inhibition Studies on Mild Steel in HCL Environment. *Surface Review and Letters* **2020**, 27 (12).
24. Salim, R. D. et al. Corrosion Inhibition of Thiadiazole Derivative for Mild Steel in Hydrochloric Acid Solution. *International Journal of Corrosion and Scale Inhibition* **2020**, 9 (2).
25. Zinad, D. S. et al. A New Synthesized Coumarin-Derived Schiff Base as a Corrosion Inhibitor of Mild Steel Surface in Hcl Medium: Gravimetric and Dft Studies. *International Journal of Corrosion and Scale Inhibition* **2020**, 9 (1).
26. Jamil, D.M. et al. Experimental and Theoretical Studies of Schiff Bases as Corrosion Inhibitors. *Chemistry Central Journal* **2018**, 12 (1).
27. Al-Amiery, A., Abdul K., Abu M., Sutiana J. A Novel Hydrazinecarbothioamide as a Potential Corrosion Inhibitor for Mild Steel in HCl. *Materials* **2013**, 6 (4).
28. Al-Amiery, A.A., F.A. Binti Kassim, A.A.H. Kadhum, and A.B. Mohamad. Synthesis and Characterization of a Novel Eco-Friendly Corrosion Inhibition for Mild Steel in 1 M Hydrochloric Acid. *Scientific Reports* **2016**, 6.
29. Kadhum, A.A.H. et al. Inhibition of Mild Steel Corrosion in Hydrochloric Acid Solution by New Coumarin. *Materials* **2014**, 7 (6).
30. Kadhim, A. et al. Corrosion Inhibitors. A Review. *International Journal of Corrosion and Scale Inhibition* **2021**, 10 (1).
31. Al-Azawi, K.F. et al. Synthesis, Inhibition Effects and Quantum Chemical Studies of a Novel Coumarin Derivative on the Corrosion of Mild Steel in a Hydrochloric Acid Solution. *Chemistry Central Journal* **2016**, 10 (1).
32. Al-Amiery, A.A. et al. Electrochemical Study on Newly Synthesized Chlorocurcumin as an Inhibitor for Mild Steel Corrosion in Hydrochloric Acid. *Materials* **2013**, 6 (12).
33. Al-Amiery, Ahmed et al. Novel Corrosion Inhibitor for Mild Steel in HCl. *Materials* **2014**, 7 (2).
34. Rubaye, A.Y.I. et al. Cheery Sticks Plant Extract as a Green Corrosion Inhibitor Complemented with LC-EIS/MS Spectroscopy. *International Journal of Electrochemical Science* **2015**, 10 (10).
35. Jamil, D.M., S.B. Al-Baghdadi, W.K. Ahmed, and A.A. Al-Amiery. 2-(1-(Benzylimino)Ethyl)Phenol as Anticorrosive Compound Supported with Quantum Chemical Calculations. *International Journal of ChemTech Research* **2016**, 9 (7).
36. Al-Amiery, A.A., and L.M. Shaker. Corrosion Inhibition of Mild Steel Using Novel Pyridine Derivative in 1 M Hydrochloric Acid. *Koroze a Ochrana Materialu* **2020**, 64 (2).
37. Hanoon, Mahdi M. et al. Corrosion Investigation of Mild Steel in Aqueous Hydrochloric Acid Environment Using N-(Naphthalen-1yl)-1-(4-Pyridinyl)Methanimine Complemented with Antibacterial Studies. *Biointerface Research in Applied Chemistry* **2021**, 11 (2).
38. Habeeb, H.J. et al. Case Study on Thermal Impact of Novel Corrosion Inhibitor on Mild Steel. *Case Studies in Thermal Engineering* **2018**, 12.
39. Junaedi, S. et al. Inhibition Effects of a Synthesized Novel 4-Aminoantipyrine Derivative on the Corrosion of Mild Steel in Hydrochloric Acid Solution Together with Quantum Chemical Studies. *International Journal of Molecular Sciences* **2013**, 14 (6).
40. Junaedi, Sutiana et al. Inhibition Effects of a Synthesized Novel 4-Aminoantipyrine Derivative on the Corrosion of Mild Steel in Hydrochloric Acid Solution Together with Quantum Chemical Studies. *International journal of molecular sciences* **2013**, 14 (6).
41. Habeeb, H.J. et al. Development of New Corrosion Inhibitor Tested on Mild Steel Supported by Electrochemical Study. *Results in Physics* **2018**, 8.
42. Salman, T.A. et al. New Environmental Friendly Corrosion Inhibitor of Mild Steel in Hydrochloric Acid Solution: Adsorption and Thermal Studies. *Cogent Engineering* **2020**,7 (1).
43. Hashim, F.G. et al. Inhibition Effect of Hydrazine-Derived Coumarin on a Mild Steel Surface in Hydrochloric Acid. *Tribologia* **2020**, 37 (3–4).
44. Alobaidy, A.H. et al. Eco-Friendly Corrosion Inhibitor: Experimental Studies on the Corrosion Inhibition Performance of Creatinine for Mild Steel in HCl Complemented with Quantum Chemical Calculations. *International Journal of Electrochemical Science* **2014**, 10 (5).
45. Obayes, H.R. et al. Quantum Chemical Assessment of Benzimidazole Derivatives as Corrosion Inhibitors. *Chemistry Central Journal* **2014**, 8 (1).
46. Sheet, Eiman Ali Ehsan et al. N-(3-Nitrobenzylidene)-2--Aminobenzothiazole as New Locally Available Corrosion Inhibitor for Iraqi Oil Industry. *Journal of the Balkan Tribological Association* **2020**, 26 (2).
47. Al-Amiery, A. A., L. M. Shaker, A. A.H. Kadhum, and M. S. Takriff. Corrosion Inhibition of Mild Steel in Strong Acid Environment by 4-((5,5-Dimethyl-3-Oxocyclohex-1-En--1-Yl)Amino)Benzenesulfonamide. *Tribology in Industry* **2020**, 42 (1).

48. Hanoon, M., D. S. Zinad, A. M. Resen, and A. A. Al-Amiery. Gravimetrical and Surface Morphology Studies of Corrosion Inhibition Effects of a 4-Aminoantipyrine Derivative on Mild Steel in a Corrosive Solution. *International Journal of Corrosion and Scale Inhibition* **2020**, 9 (3).
49. Yamin, J. A.A., E. Ali Eh Sheet, and A. Al-Amiery. Statistical Analysis and Optimization of the Corrosion Inhibition Efficiency of a Locally Made Corrosion Inhibitor under Different Operating Variables Using RSM. *International Journal of Corrosion and Scale Inhibition* **2020**, 9 (2).
50. Al-Taweel, S. S., T. S. Gaaz, L. M. Shaker, and A. Al-Amiery. Protection of Mild Steel in H_2SO_4 Solution with 3-((3-(2-Hydroxyphenyl)-5-Thioxo-1,2,4-Triazol-4-Yl) Imino)Indolin-2-One. *International Journal of Corrosion and Scale Inhibition* **2020**, 9 (3).
51. Al-Amiery, Ahmed A. Anti-Corrosion Performance of 2-Isonicotinoyl-n-Phenylhydrazinecarbothioamide for Mild Steel Hydrochloric Acid Solution: Insights from Experimental Measurements and Quantum Chemical Calculations. *Surface Review and Letters* **2021**, 28 (3).
52. Shaker, Lina M., Aqeel Al-Adili, Ahmed A. Al-Amiery, and Mohd S. Takriff. The Inhibition of Mild Steel Corrosion in 0.5 M H_2SO_4 solution by N-Phenethylhydrazinecarbothioamide (N-PHC). *Journal of Physics: Conference Series* **2021**, 1795 (1).
53. Kadhim, Abdulhadi et al. Synthesis and Characterization of Triazol Derivative as New Corrosion Inhibitor for Mild Steel in 1M HCl Solution Complemented with Antibacterial Studies. *Journal of Physics: Conference Series* **2021**, 1795 (1).
54. Al-Baghdadi, S.B. et al. Synthesis and Corrosion Inhibition Application of NATN on Mild Steel Surface in Acidic Media Complemented with DFT Studies. *Results in Physics* **2018**, 8.
55. Jawad, Q. A. et al. Synthesis and Comparative Study of Novel Triazole Derived as Corrosion Inhibitor of Mild Steel in HCl Medium Complemented with DFT Calculations. *International Journal of Corrosion and Scale Inhibition* **2020**, 9 (2).
56. Obayes, H.R. et al. Sulphonamides as Corrosion Inhibitor: Experimental and DFT Studies. *Journal of Molecular Structure* **2017**, 1138.
57. Al-Baghdadi, S et al. Experimental Studies on Corrosion Inhibition Performance of Acetylthiophene Thiosemicarbazone for Mild Steel in HCl Complemented with DFT Investigation. *International Journal of Low-Carbon Technologies* **2021**, 16 (1).
58. Resen, A.M. et al. Gravimetrical, Theoretical, and Surface Morphological Investigations of Corrosion Inhibition Effect of 4-(Benzoimidazole-2-Yl) Pyridine on Mild Steel in Hydrochloric Acid. *Koroze a Ochrana Materialu* **2020**, 64 (4).
59. Al-Amiery, Ahmed A., Yasmien K. Al-Majedy, Haziem Abdulreazak, and Hussain Abood. Synthesis, Characterization, Theoretical Crystal Structure, and Antibacterial Activities of Some Transition Metal Complexes of the Thiosemicarbazone (Z)-2-(Pyrrolidin-2-Ylidene)Hydrazinecarbothioamide. *Bioinorganic Chemistry and Applications* **2011**.
60. Yousif, E. et al. Furosemide as an Environmental-Friendly Inhibitor of Corrosion of Zinc Metal in Acid Medium: Experimental and Theoretical Studies. *International Journal of Electrochemical Science* **2015**, 10 (2).
61. Zinad, D. S. et al. Adsorption, Temperature and Corrosion Inhibition Studies of a Coumarin Derivatives Corrosion Inhibitor for Mild Steel in Acidic Medium: Gravimetric and Theoretical Investigations. *International Journal of Corrosion and Scale Inhibition* **2020**, 9 (1).
62. Al-Baghdadi, Shaimaa B., Ahmed A. Al-Amiery, Abdul A. Kadhum, and Mohd Sobri Takriff. Computational Calculations, Gravimetrical, and Surface Morphological Investigations of Corrosion Inhibition Effect of Triazole Derivative on Mild Steel in HCl. *Journal of Computational and Theoretical Nanoscience* **2020**, 17 (11).